16th World Conference on Earthquake, 16WCEE 2017
Santiago Chile, January 9th to 13th 2017
Paper N° 625
Registration Code: S-U1460339799

NUMERICAL SIMULATION OF THE SEISMIC RESPONSE OF CAISSON QUAY WALLS ON LIQUEFIABLE SOIL

J-S. Lee[(1)], G-D. Noh[(2)], M-T. Yoo[(3)]

[(1)]Associate Professor, Wonkwang University, blueguy@wku.ac.kr
[(2)]Engineer, Hanmac Engineering & Consultant; Former Graduate Student, Wonkwang University, epic.no.7@gmail.com
[(3)]Senior Researcher, Korea Railroad Research Institute, thezes03@krri.re.kr

Abstract

Engineers and researchers have reached a consensus to adopt a performance-based design of port and harbor structures in Japan after a hazard investigation of the 1995 Kobe earthquake. The critical success factor for implementing a performance-based earthquake-resistant design depends on the reliable estimation of permanent displacement after an earthquake. The non-linear explicit response history analysis (NERHA) is presently the most efficient method used to predict the soil–foundation–structure interaction response. This study aims to rigorously verify the NERHA using well-defined field measurements, existing numerical tools, and constitutive models. The Port Island site in Kobe provides intensive hazard investigation data, strong motion records of downhole seismic arrays, and sufficient engineering parameters of soil before the earthquake. The analysis result matches quite well with the field investigation records. The NERHA procedure presented in this paper can be used in further studies to explain and examine the effects of other factors on the seismic behavior of gravity quay walls lying on a liquefiable soil area.

Keywords: performance-based design; effective stress analysis; numerical analysis; liquefaction; quay wall

1. Introduction

A 7.2-magnitude earthquake struck the Port of Kobe on Tuesday, January 17, 1995. The Port of Kobe, which is one of the largest container terminal facilities in the world, was practically destroyed. Port Island, which is a human-made container terminal constructed by land reclamation, was nearly completed when the earthquake struck. The predominant damage to the concrete caisson quay walls was a result of soil liquefaction and lateral spreading. A number of quay walls rotated and slid. The residual horizontal displacement at the top of the quay walls reached up to 3 m. Researchers reached a consensus to adopt a performance-based design in the port and harbor structures of Japan after the hazard investigation of the Kobe earthquake.

The residual displacement of geotechnical structures after an earthquake is one of the most important engineering demands in performance-based earthquake-resistant designs. Therefore, providing reliable responses of geotechnical structures using various techniques after an earthquake is essential. The non-linear explicit response history analysis (NERHA) of geotechnical structures is presently the most efficient method used to achieve this goal. However, performing a laboratory-scale verification of effective stress analysis, including post liquefaction behavior, is difficult. Therefore, this study aims to rigorously verify the NERHA using well-defined field measurements, existing numerical tools, and constitutive models. The Port Island site provides intensive hazard investigation data, strong motion records of downhole seismic arrays up to 82 m depth, and sufficient engineering parameters of subsoils before the 1995 earthquake. Many researchers employed numerical analyses to simulate the hazard, which occurred in the man-made island after the 1995 earthquake. The main issue to tackle was representing the complex behavior of the saturated sandy soil in a numerical analysis. Previous researchers introduced their own unique constitutive soil models or combined existing constitutive models. The analysis results show a reasonable agreement with the hazard investigation data regardless of the constitutive model adopted. Therefore, the previous numerical simulation work on Port Island has its own identity (Table 1).

Table 1 – Previous numerical simulations on the caisson quay wall during the 1995 Kobe earthquake

Researchers	Method(Program)	Constitutive model
Iai et al. (1998) [1] Sawada et al. (2000) [2]	FEM(FLIP)	Cyclic mobility Multi yield spring model
Yang (1999) [3]	FDM(FLAC)	Linear elastic and simple liquefaction model
Dakoulas and Gazetas(2005) [4]	FDM(FLAC)	Pastor et al. [9]
Alyami et al. (2007) [5]	FEM(UWLC)	Pastor et al. [9]
Na et al. (2008, 2009) [6][7]	FDM(FLAC)	Linear elastic/Finn and Byrne liquefaction model
Galavi et al. (2013) [8]	FEM(Plaxis)	UBC 3D-PLM Sand model

This study aims to ensure the robustness of the conventional methods used in the seismic design procedure by verifying the numerical analysis based on historical earthquake hazard investigation data. These methods include site investigation, numerical analysis, and implementation procedure of soil properties. The NERHA is conducted using the commercial numerical analysis tool, FLAC 2D. This tool analyzes non-linear cyclic soil behavior using an explicit time integration method in Lagrangian coordinates. A 2D finite difference model is constructed under a plane strain condition. The strong motion data recorded at 82 m depth are used as a command motion for the rigid bottom boundary. Soil is modeled to represent hysteretic energy dissipation using the Mohr–Coulomb failure criterion. The liquefiable soil strata, backfill, and replaced sand beneath the caisson are modeled using liquefaction models. The estimated horizontal residual displacement shows a reasonable agreement with historical measurements. Subsequently, the liquefaction model effect is examined. The NERHA procedure presented in this paper can be used in further studies to explain and examine the effects of other factors on the seismic behavior of gravity quay walls lying on a liquefiable soil area.

2. 1995 Kobe earthquake and man-made island

The Port and Rokko islands, which were designed for use as a container terminal and a waterfront space, respectively, were two of the most damaged industrial facilities in 1995. These islands were located 17 km away from the epicenter and reclaimed with soil excavated from the Rokko mountain area. The island perimeters were constructed using concrete caisson. Soil reclamation, often called Masado, was commonly observed in the far-east area and classified as silty sand (SM) by the Unified Soil Classification System. Fig. 1 shows the Masado grain size distribution curve. Some Masado particles lie in the liquefiable grain size distribution range. However, the soil above the dredging level was reclaimed without employing the densification process [10].

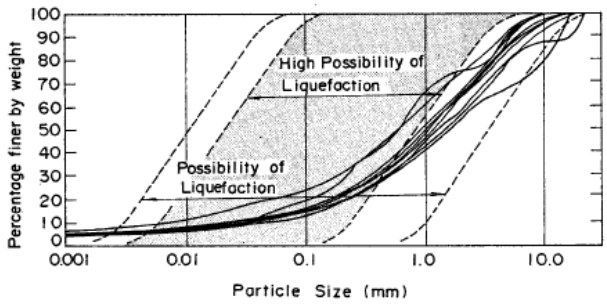

Fig. 1 – Grain size distribution of Masado [11]

The construction project was divided into three sectors, namely, Port Island phases I and II and Rokko Island (Fig. 2). Different soft soil improvement methods were adopted for each phase. Therefore, each phase had different section profiles [11]. An intensive site investigation was conducted throughout the construction area before the 1995 earthquake. Fig. 2 illustrates the in-situ logging location and sampling spot. Dynamic soil properties were obtained from in-situ logging and laboratory tests. Fig. 3 shows the representative subsoil profile, the standard penetration test (SPT) N-value of Port Island phase I, and the installation elevation of the vertical seismic array. The strong earthquake component struck in the north–south direction. Fig. 4 shows corrected

accelerograms recorded at the vertical seismic array station. The motion at 83 m depth was corrected because of the seismograph rotation during the earthquake [13].

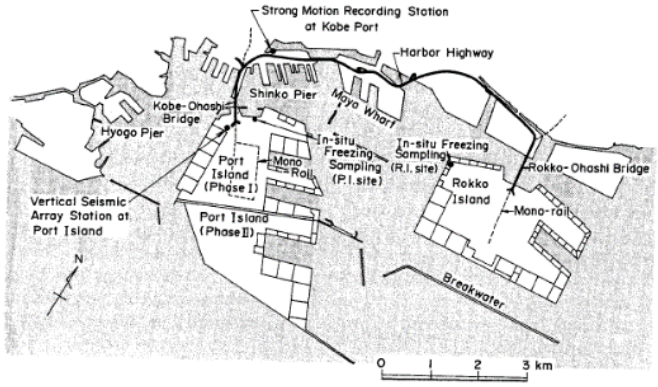

Fig. 2 – Plan of Kobe port, location of seismic array and in-situ test and sampling spot [11]

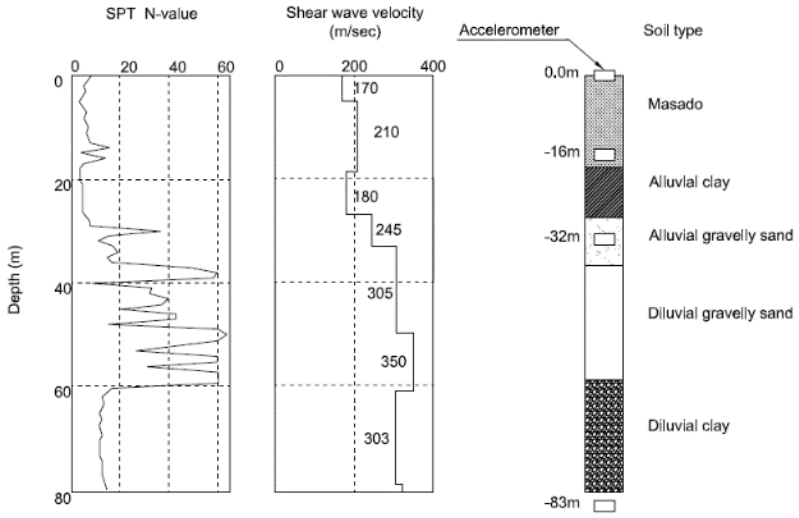

Fig. 3 – Subsoil profile(before earthquake) and location of the vertical seismic array (After [12])

The reclaimed soil behind the caisson quay wall was widely liquefied during the earthquake. This phenomenon dramatically increased the lateral earth pressure and the overturning moment acting on the quay walls. These increments resulted in the bearing capacity failure around a caisson toe. The consequence of the bearing capacity failure was observed as a permanent displacement of the concrete caisson. The maximum and average permanent horizontal displacement was observed to be 5 m and 3 m, respectively, whereas the maximum and average permanent vertical displacement was observed to be 2.5 m and 1.5 m, respectively [11].

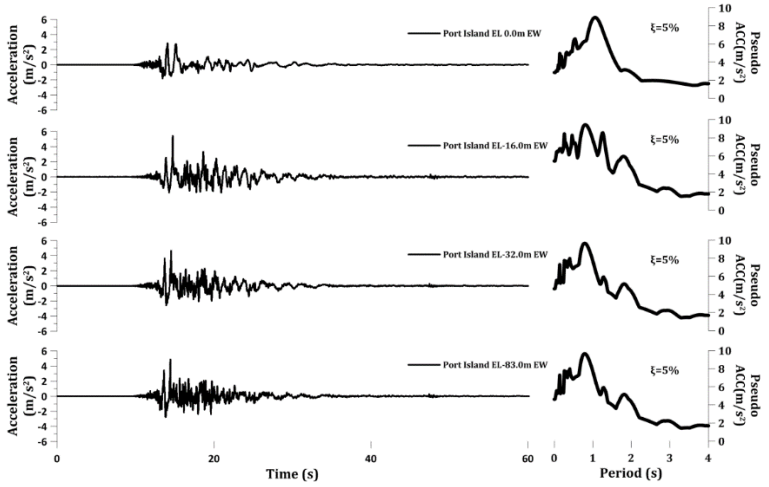

Fig. 4 – Horizontal acceleration histories recorded at the vertical seismic array located in Port Island phase I

3. Numerical analysis

The numerical integration in a dynamic analysis can be executed using two methods, namely, implicit and explicit. These two methods have their own advantages. However, the explicit method is more suitable for solving non-linear transient problems [14, 15]. This study used FLAC 2D, which was developed by the Itasca Consulting Group, to simulate the caisson quay wall response at Port Island during the 1995 Kobe earthquake. The program solved partial differential equation problems using the finite difference method in the explicit method [16]. The section profile of the target caisson (i.e., PC-I) near the vertical seismic array was numerically modeled under the plane strain condition (Fig. 5).

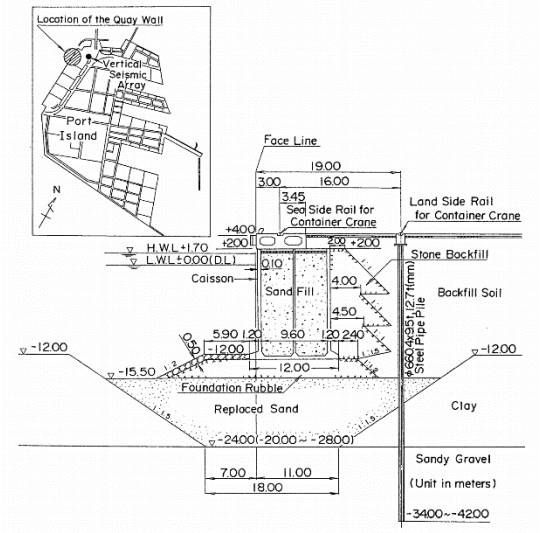

Fig. 5 – Cross section of a quay wall at Port Island PC-I [11]

The entire model size had a 180 m and 80 m dimension in the horizontal and vertical directions, respectively. The concrete caisson was modeled as an elastic material, whereas the others were modeled as elastoplastic. The earthquake energy trapping inside the horizontal boundary was minimized by attaching free-field elements along the boundary. The rigid base boundary condition that reflects the whole waves traveling

downward with opposite polarity was used as an input motion boundary. The rigid base condition may accumulate inherent error, but it was the best means of using the within motion as an input motion record [17]. Eq. (1) was utilized to compute the maximum diagonal length of the finite difference grid (i.e., 2.1 m) [18]. Therefore, the whole model was able to transmit the wave energy below 11.3 Hz.

$$\Delta l \leq \frac{\lambda}{10}, f \leq \frac{v_s}{10 \times \Delta l} \quad (1)$$

where Δl is the spatial element size; λ and f are the wavelength and frequency associated with the highest frequency component containing appreciable energy, respectively; and v_s is the shear wave velocity.

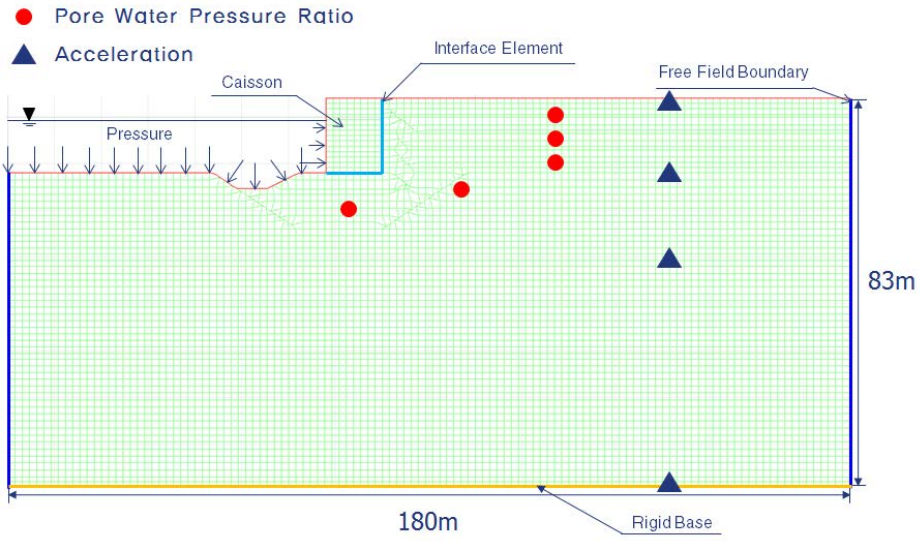

Fig. 6 – Dimension, boundary conditions and measurement of the numerical model

The static water pressure acting on the caisson surface and the seabed was applied as a distributed pressure. The pore-water pressure distribution below the ground water table was calculated and updated using seepage analysis at each construction step. The concrete caisson and the surrounding soils were attached using interface elements that separated the two different materials upon exertion of excessive stress. The interface element showed a perfect elastic–perfect plastic behavior for both normal and shear stresses. Accordingly, this study used two soil constitutive model types. Before failure, soil behaved as a non-linear elastic material obeying the Masing rule [19] under the cyclic loading condition. After failure, the model follows the associative flow rule based on the Mohr–Coulomb failure criteria. The Byrne model [20] was also used for the liquefaction-susceptible soil layers. This model accounted for excess pore-water pressure induced by the volumetric strain changes according to load reversal counts. The soil non-linearity was fitted using the mathematical hyperbolic model [21]. Fig. 7 shows the non-linear soil layer characteristics and the fitting results from the laboratory sample tests obtained before the 1995 earthquake. Table 2 summarizes the other engineering properties of soil. These properties were compared and selected based on previously published studies [12, 23, 24, 25, 26]. The SPT N-values obtained were corrected to an energy efficiency of 78% [11] and overburden pressure.

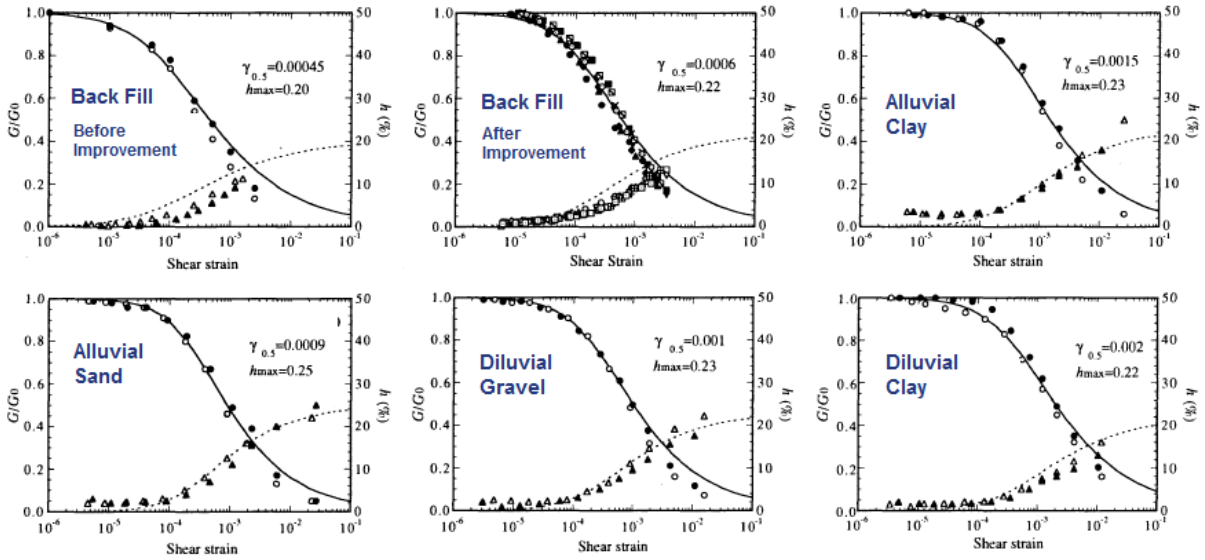

Fig. 7 – Nonlinearity and cyclic damping characteristics of soil (After [22])

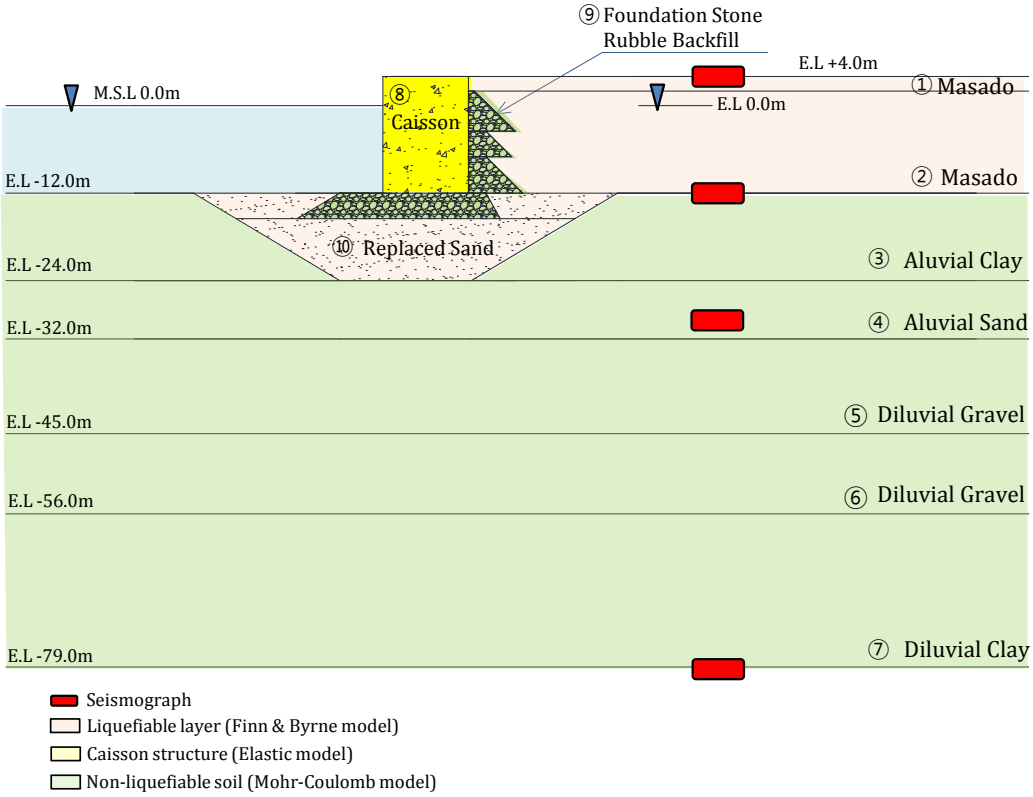

Fig. 8 – Soil layer, constitutive model block and corresponding engineering properties in Table 2.

The analysis was conducted using the following construction steps to account for the initial soil layer stress condition: (1) natural ground level, (2) excavation for foundation replacement, (3) caisson placement, and (4) backfill behind the caisson. The above-mentioned analysis was executed under the Euler coordinate (small strain) system. The settlement after the concrete caisson placement was about 1.3 cm. The additional

displacements after the backfill were 0.2 cm and 0.7 cm in the horizontal and vertical directions, respectively. These values were quite reasonable as compared with similar construction project records. The successive dynamic analysis was conducted under the stress condition of the final step. The whole numerical model was changed into a Lagrangian coordinate (large strain) system to account for the geometric non-linearity that occurred because of the position changes of the center of gravity. Another numerical damping was used in addition to inherent hysteretic material damping to generate minimum soil damping and reduce high-frequency numerical noises. The analysis results were interpreted in time histories in terms of acceleration, displacement, and pore-water pressure. The locations of the acceleration measurement points of the numerical analysis were identical with those of the physical measurement points.

Table 2. Selected engineering soil parameters of Port Island for the numerical analysis

Layer	Dry density (kg/m^3)	V_s (m/s)	Bulk modulus* (Pa)	Permeability (m/s)	Average SPT N value		Poisson's ratio	Notation
					N	N_{60}**		
Masado	1,800	170	8.7×10^{7}	4.0×10^{-6}	36	7.3	0.25	①
	1,800	210	1.3×10^{8}	1.0×10^{-9}	36	9.2	0.25	②
Alluvial clay	1,600	180	1.1×10^{8}	1.0×10^{-12}	3.5	4.9	0.3	③
Alluvial sand	1,800	245	1.8×10^{8}	1.0×10^{-9}	13.5	19.1	0.25	④
Diluvial gravel	1,850	305	2.9×10^{8}	1.0×10^{-6}	36.5	51.7	0.25	⑤
	1,850	350	3.8×10^{8}	1.0×10^{-6}	61.9	87.6	0.25	⑥
Diluvial clay	1,600	303	3.2×10^{8}	1.0×10^{-12}	11.7	16.5	0.3	⑦
Caisson	1,920***	-	1.4×10^{10}	-	-	-	0.2	⑧
Foundation stone/Rubble	2,000	-	2.1×10^{8}	1.0×10^{-4}	-	-	0.3	⑨
Replaced Soil	1,800	-	2.4×10^{8}	1.0×10^{-10}	-	28.3	0.3	⑩

*Maximum bulk modulus are calculated based on shear wave velocity and Poisson's ratio
**Corrected N Value : Overburden pressure 98kPa, Energy efficiency 78% [11]
***Equivalent dry density (Concrete and inside fill materials)

4. Analysis results

4.1 Acceleration time history

Liquefaction was one of the most significant phenomena in the 1995 Kobe earthquake. Liquefaction occurred along the shore side and the water front structure. Consequently, the increased damping suppressed the amplification of the earthquake motion that traveled in the upward direction. Fig. 9 shows a direct comparison of the acceleration time histories obtained from the numerical analysis results and the in-situ records. The time histories obtained from the numerical analysis results broadly follows the in-situ records. However, the wave energy around 1 Hz diminishes faster than in the in-situ record, which may have been caused by the behavioral accuracy of the liquefaction model used in post-liquefaction stages in this study.

4.2 Permanent caisson displacement

Permanent displacement played important roles in deciding on the performance goal of port and harbor structures. Therefore, checking the estimated permanent displacement accuracy was important to ensure the reliability of the numerical analysis technique. Fig. 10 displays the permanent displacements of the concrete caisson (i.e., PC-I) in Port Island after the Kobe earthquake shock along with the result obtained from the numerical analyses.

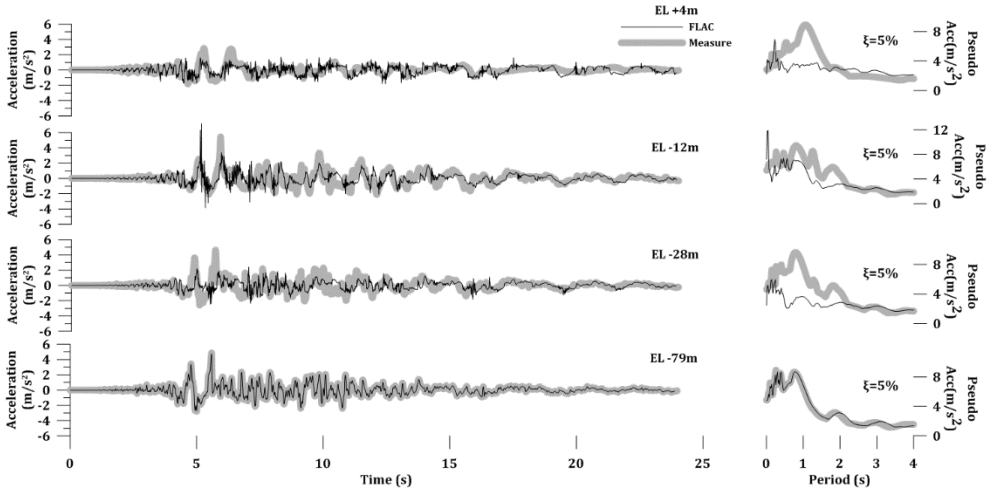

Fig. 9 – Comparison of acceleration time histories

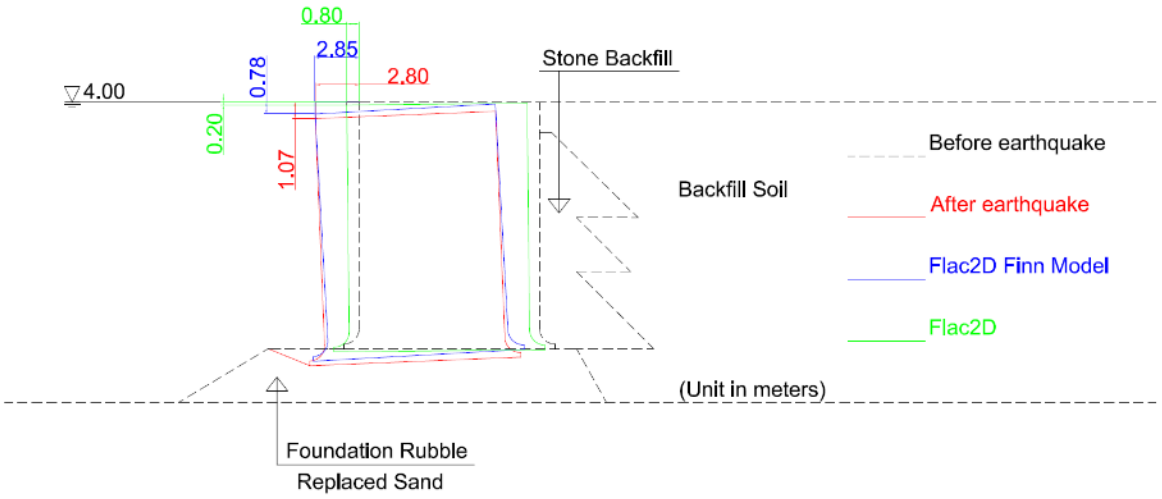

Fig. 10 – Permanent displacement of the quay caisson wall PC-I (Measurement, Numerical analysis)

The numerical analysis results agreed quite well with the measurement data when the liquefaction model was used (blue line, Fig. 10). However, the numerical analysis yielded a much smaller displacement without the liquefaction model (green line, Fig. 10). In other words, the liquefaction model should be used in conducting an effective stress analysis upon deciding on the performance goal of port and harbor structures lying on liquefaction-susceptible areas.

The overall quay wall movement was induced by an increase in the lateral earth pressure acting behind the quay walls. The main cause of this increment was liquefaction. The liquefaction phenomenon increased the active earth pressure coefficient up to 1.0. Therefore, the total thrust acting on the wall might have increased three times. The increased thrust resulted in the overturning moment and bearing pressure increment at the front edge of the quay caisson base. Consequently, the bearing capacity failure occurred beneath the quay wall toe because of the bearing pressure increment and the seismic bearing capacity decrement [27, 28]. An underwater

investigation conducted by divers showed evidence of the bearing capacity failure in the shape of a seabed uplift in front of the quay caisson (Fig. 11) [11]

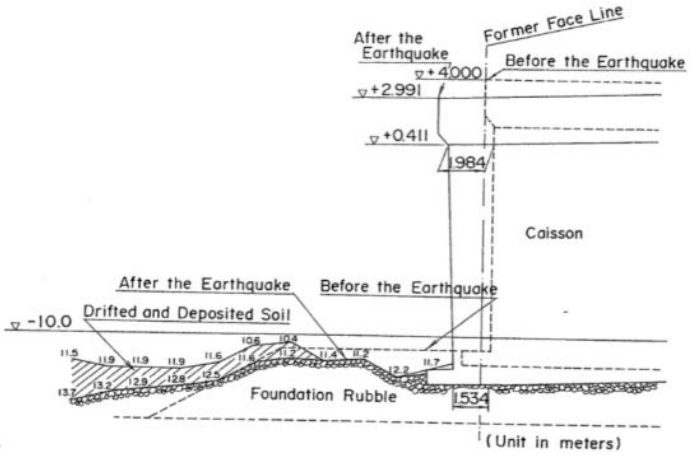

Fig. – 11 Deformation of rubble mound in front of the quay caisson [11]

The failure mechanism was also found in the numerical analysis. Fig. 12 simultaneously shows the shear strain increment and the displacement vector. The shear strength failure of soil was easily identified using this process. A very similar failure mechanism with the actual cases was also observed. However, this mechanism cannot be spotted when the analysis was conducted without the liquefaction soil constitutive model.

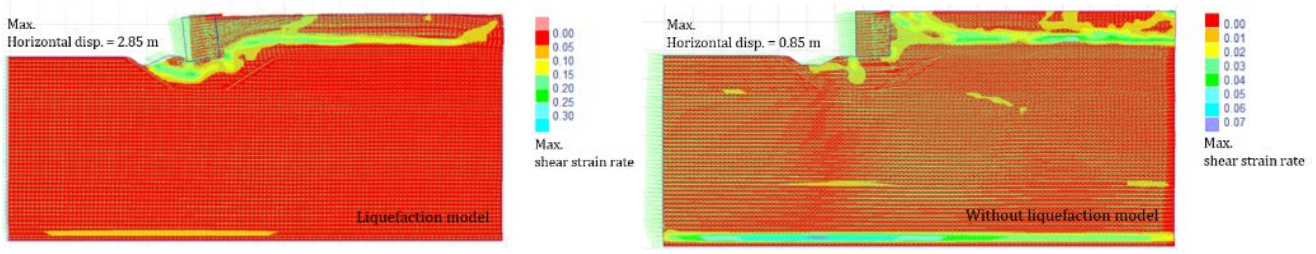

Fig. – 12 Failure mechanism of concrete caisson quay wall in the numerical analysis

4.2 Pore-water pressure and calculation time

Fig. 13(a) shows the maximum excess pore-water pressure ratio during the entire excitation period, which was stored in memory and expressed as a distribution contour. Accordingly, Eq. (2) was used to calculate the ratio. Liquefaction was presumed to occur in the area where the excess pore-water pressure ratio exceeded 1.0. The backfill soil behind the quay wall and the replaced sand under the rubble mound seem to be completely liquefied. Fig. 13(b) plots the corresponding excess pore-water pressure ratio histories. No pore-water pressure transducer was installed in the Port Island area. Therefore, the accuracy of the excess pore-water pressure ratio history cannot actually be judged. However, the histories were helpful in understanding the pore-water pressure accumulation mechanism during shaking. Most of the excess pore-water pressure was generated and accumulated until the first large shaking hit the site. The pressures were redistributed or retained thereafter regardless of the subsequent shaking. Analysis was conducted under the undrained condition. Therefore, redistribution was conducted through soil volume change following the geometric deformation of the whole model and not by using the seepage process.

$$R_u = \frac{\mathrm{u}}{\bar{\sigma}_{v0}} \tag{2}$$

where u is pore-water pressure, $\bar{\sigma}_{v0}$ is effective overburden pressure before earthquake

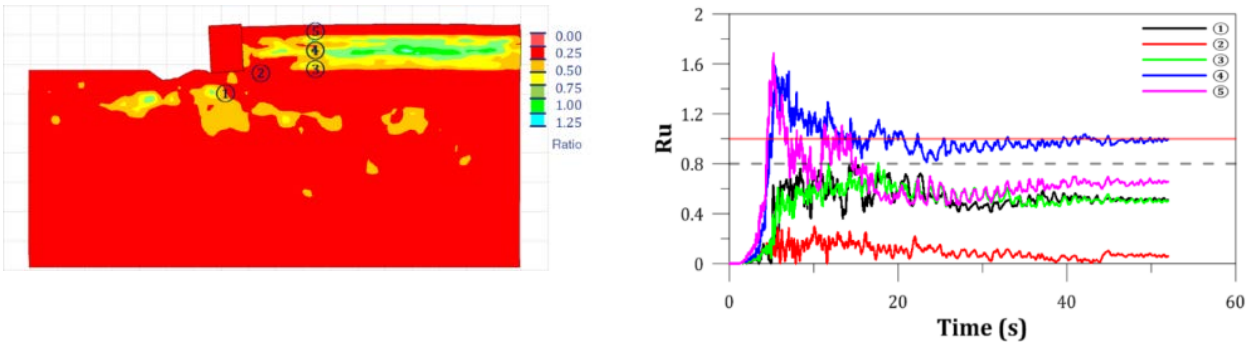

(a) Max. excess pore-water pressure ratio contour (b) Computed time histories

Fig. – 13 Excess pore-water pressure contour and time histories

The time-domain effective stress analysis was stereotyped as time consuming and unrealistic for use in the design process. However, this time-consuming disadvantage has now been avoided with the help of the development in the computer industry and computing algorithm. The numerical analysis program used in this study employed multi-core processing and dynamic multi-stepping techniques [16]. These techniques effectively reduced the computing time. The required analysis time was about 4 h when a single Intel Xeon E5-2699v3 processor was used. This processor had 18 cores and 36 threads operating at a 2.3 GHz clock speed.

5. Conclusion

This study performs a rigorous verification of the non-linear effective stress analysis based on the measurement data obtained from the Port Island site in Japan during the 1995 Kobe earthquake. The site is an ideal location to perform the verification process with the help of abundant site investigation data and hazard investigation and earthquake motion records obtained from a vertical seismic array. Before failure, the soil constitutive model used in this study behaves as a non-linear elastic material that obeys the Masing rule under the cyclic loading condition. After failure, the model follows the associative flow rule based on the Mohr–Coulomb failure criteria. The liquefaction model is used for the liquefaction-susceptible layers. None of the engineering parameters used to construct the numerical model are special; these parameters are only general parameters that can be obtained from an ordinary site investigation process. The permanent displacements of the concrete caisson quay wall are almost identical in the numerical simulation and the historical records when the liquefaction soil constitutive model is used. Therefore, the verified numerical technique can be utilized to estimate the performance goal in a performance-based earthquake resistance design and in further parametric studies.

6. Acknowledgements

This research was supported by Basic Science Research Program through the National Research Foundation of Korea(NRF) funded by the Ministry of Education(2014R1A1A2055195) and by a grant (15RTRPB067919-03) from Railroad Technology Research Program funded by Ministry of Land, Infrastructure and Transportof Korean government

7. Copyrights

8. References

[1] Iai S, Ichii K, Liu H, Morita T (1998): Effective stress analyses of ports structures. *Soil and Foundations*, **38** (SP), 97-114.

[2] Sawada S, Ozutsumi O, Iai S (2000): Analysis of liquefaction induced residual deformation for two types of quay walls – Analysis by "FLIP". *12th World Conference on Earthquake Engineering 12WCEE*, Auckland, New Zealand.

[3] Yang D-S (1999): Deformation-Based Seismic Design Models for Waterfront Structures. *Ph. D Dissertation*, Oregon State University, USA.

[4] Dakoulas P, Gazetas G (2005): Seismic effective-stress analysis of caisson quay walls - application to Kobe. *Soil and Foundations*, **45** (4), 133-147.

[5] Alyami M, Wilkinson SM, Rouainia M, Cai F (2007): Simulation of seismic behavior of gravity quay wall using a generalized plasticity model. *4th International conference on earthquake geotechnical engineering 4ICEGE*, Thessaloniki, Greece.

[6] Na UJ, Chaudhuri SR, Shinozuka M (2008): Probabilistic assessment for seismic performance of port structures. *Soil Dynamics and Earthquake Engineering*, **28** (2), 147-158.

[7] Na UJ, Chaudhuri SR, Shinozuka M (2009): Effects of spatial variation of soil properties on seismic performance of port structures. *Soil Dynamics and Earthquake Engineering*, **29** (3), 537-545.

[8] Galavi V, Petlas A, Brinkgreve BJ (2013): Finite element modelling of seismic liquefaction in soils. Geotechnical Engineering Journal of the SEAGS & AGSSEA, **44** (3), 55-64.

[9] Pastor M, Zienkiewicz O, Chan CH (1990): Generalized plasticity and the modeling of soil behavior. International Journal of Numerical and Analytical Methods in Geomechanics, **14**, 151-190

[10] Ishihara K (1997): Terzaghi oration – Geotechnical aspects of the 1995 Kobe earthquake. *Proceedings of International Conference on Soil Mechanics and Foundation Engineering ICSMFE*, Hamburg, Germany, pp 2047-2073.

[11] Inagaki H, Iai S, Sugano T, Yamazaki H, Inatomi T (1996): Performance of caisson type quay walls at Kobe port. *Soil and Foundations*, **36** (SP), 119-136.

[12] Cubrinovski M, Ishihara K, Tanizawa F (1996): Numerical simulation of the Kobe port island liquefaction. *11th World Conference on Earthquake Engineering 11WCEE*, Acapulco, Mexico.

[13] Ansary MA, Yamazaki F, Katayama T (1997): Analysis of ground motions at a reclaimed site during the 1995 great Hanshin earthquake. Journal of Civil Engineering, The Institute of Engineers, Bangladesh, **CE25** (1), 79-95

[14] Dokanish MA, Subbaraj K (1989): A survey of direct time-integration methods in computational structural dynamics – I. Explicit methods. Computers and Structures, **32** (6), 1371-1386.

[15] Dokanish MA, Subbaraj K (1989): A survey of direct time-integration methods in computational structural dynamics – II. Implicit methods. Computers and Structures, **32** (6), 1387-1401.

[16] Itasca CG (2015): User's Manual, FLAC-Fast Lagrangian Analysis of Continua. Itasca Consulting Group.

[17] Mejia LH, Dawson EM (2006): Earthquake deconvolution for FLAC. *Proceedings of 4th international FLAC symposium on numerical modeling in geomechanics*, Madrid, Spain.

[18] Kuhlemeyer RL, Lysmer J (1973): Finite element method accuracy for wave propagation problems. *Journal of Soil Mechanics and Foundation Engineering Division ASCE*, 99 (5), 421–427.

[19] Masing G (1926): Eigenspannungen und verfestigung beim messing. *Proceedings of the second international congress of applied mechanics*, 332–335.

[20] Byrne P (1991): A cyclic shear-volume coupling and pore-pressure model for sand. *Proceedings of 2nd international conference on recent advances in geotechnical earthquake engineering and soil dynamics*, St. Louis, USA, 47-55.

[21] Hardin BO, Drnevich VP (1972): Shear modulus and damping in soils - design equation and curves. *Journal of Soil Mechanics and Foundation Engineering Division ASCE*, **98** (7), 667–691.

[22] Fujikawa S, Fukutake K (2001): Simulation of the vertical seismic array records at the Kobe port island considering the effect of the improved ground adjacent to the array site. *Journal of Japanese Society of Civil Engineering JSCE*, **687** (III-56),169-180

[23] Kazama M, Yamaguchi A, Yanagisawa E (1998): Seismic behavior of an underlying alluvial clay on man-made islands during the 1995 Hyogoken-Nambu earthquake, *Soil and Foundations*, **38** (SP), 23-32.

[24] Iwasaki Y, Tai M (1996): Strong motion records at Kobe port island. *Soil and Foundations*, **36** (SP), 29-40.

[25] Madabhushi SPG (1995): Strong motion at port island during the Kobe earthquake. *Technical Report*. Cambridge University, Department of Engineering.

[26] Shiomi T, Mutsuhiro Y (1996): Effect of multi-directional loading and initial stress on liquefaction behavior. *11th World Conference on Earthquake Engineering 11WCEE*, Acapulco, Mexico.

[27] Richards R, Elms DG, Budhu M (1993): Seismic bearing capacity and settlements of foundations. *Journal of Geotechnical Engineering ASCE*, **119** (4), 662-674.

[28] Paolucci R, Pecker A (1997): Seismic bearing capacity of shallow strip foundations on dry soils. *Soil and Foundations*, **37** (3), 95-105.